Temperature quench echoes in proteins

Dong Xu and Klaus Schulten

Department of Physics and Beckman Institute, University of Illinois at Urbana–Champaign, Urbana, Illinois 61801

Oren M. Becker[a) and Martin Karplus

Department of Chemistry, Harvard University, Cambridge, Massachusetts 02138

Temperature quench echoes are analyzed in terms of the temperature–temperature correlation function in the harmonic approximation, and the resulting expressions are compared with molecular dynamics simulations. The relationship between the time dependence of the echo depth and the density of states is demonstrated for harmonic systems. For a protein, which has significant anharmonicity, the time dependence is dominated by relaxation effects that originate from dephasing of the periodic motions. A simple relaxation model is shown to provide a good description of the results observed in the simulations. © *1995 American Institute of Physics.*

I. INTRODUCTION

Molecular dynamics simulations of biopolymers are now being widely used to study their structure, dynamics and thermodynamics.[1,2] Certain properties are difficult to visualize directly. Some of these can be revealed through numerical experiments which apply sudden perturbations and monitor the response. The temperature quench echo is a good example. Temperature quench echoes were first observed in simulations of a Lennard-Jones glass by Grest *et al.*[3] and were demonstrated recently in a protein, the bovine pancreatic trypsin inhibitor (BPTI).[4] A typical quench echo is shown in Fig. 1. A molecular dynamics simulation of a system equilibrated at a certain temperature is halted at time $t=0$ and then continued with the same positions, but with zero velocities for all particles. This procedure, which creates a coherent system, is referred to as a quench. The same quench is applied a second time at $t=\tau$. The echo manifests itself as a brief decrease in the kinetic energy or, according to the relationship

$$T=\frac{2}{3k_B N}\sum_i \frac{1}{2}m_i \mathbf{v}_i^2 \quad (N=\text{number of atoms}) \quad (1)$$

as a dip in the temperature T of the system.

Rahman and co-workers provided an interpretation of the quench echo phenomenon and showed how it could be used to study various aspects of the dynamics of a Lennard-Jones glass.[3,5–7] The authors formulated their analysis in the harmonic approximation, which was also employed in Ref. 4 to interpret echoes in proteins. In the present paper we reformulate the harmonic description in terms of the temperature-temperature correlation function. This provides a basis for a more detailed study of the properties of the temperature quench echoes. The results are compared to simulations of model systems and to molecular dynamics calculations of the protein BPTI.

In Refs. 3 and 4 it was suggested that the echo depth provides an estimate of the density of states. We show here that although the echo depth is related to the density of states, the relationship is more complex than initially assumed. We demonstrate that vibrational dephasing due to the anharmonicity of the protein plays a dominant role in the decay of the echo depth with increasing time.

In Section II we describe briefly the molecular dynamics algorithm employed. Section III presents a description of the temperature echo phenomenon within the harmonic approximation and shows how it can be expressed in terms of the temperature–temperature correlation function. In Section IV, the exact relation of the echo depth to the density of states is derived and illustrated. Section V uses a simple model to examine anharmonicity effects on the temperature echo. In Section VI, we summarize and discuss the results.

II. METHODS

The simulation for BPTI underlying Fig. 1 is basically a repetition of the work presented in Ref. 4. BPTI has 58 amino acids and 898 atoms in an all atom model. We used a well equilibrated structure obtained by molecular dynamics simulations at 300 K in vacuum of about 1 ns starting from the 1.5 Å resolution x-ray structure.[8] To prepare the coordinates at $t=0$ in Fig. 1, a 15 ps molecular dynamics simulation at 300 K was carried out. During the first 5 ps of the simulation, the protein was coupled to a heat bath at 300 K by rescaling velocities through[9]

$$v_i^{\text{new}}=v_i^{\text{old}}\sqrt{1-\lambda+\lambda T_0/T}, \quad (2)$$

where $T_0=300$ K, $\lambda=0.01$ and T is the temperature defined in Eq. (1). During the remaining 10 ps, no coupling to a heat bath was applied. The average temperature during the period 10 ps$<t<$15 ps was $T_0=297.86$ K with fluctuations of ± 5.67 K. We employed the coordinates at 10, 11, 12, 13, 14 and 15 ps to simulate six temperature quench echoes. The temperatures shown in Fig. 1 and Fig. 3 below were an average over these six quench echo simulations. The simulations were carried out using the molecular dynamics package MD/PMD with the fast multipole approximation (FMA) to

---

[a)Present address: School of Chemistry, Tel Aviv University, Tel Aviv 69978, Israel.
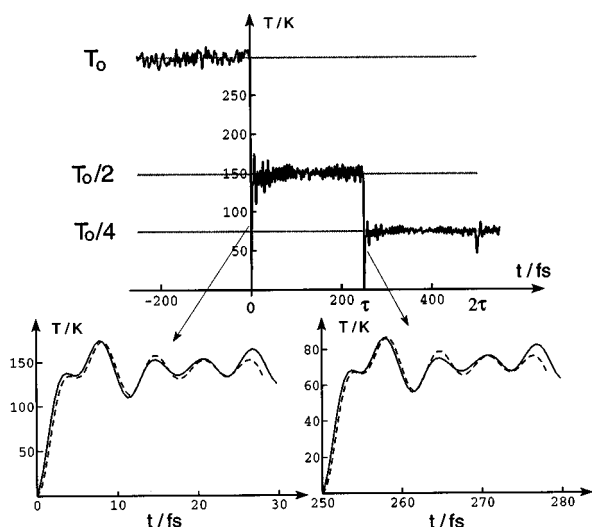
FIG. 1. Double quench, quench echo and comparison with the temperature-temperature correlation function $C_{T,T}(t)$ [see Eq. (15)]. The solid lines represent results averaged over six simulations for the protein BPTI; the dashed lines are predictions due to the harmonic model, i.e., Eq. (24) and Eq. (31). The bottom diagrams are enlargements of the top diagram. The first quench was applied at $t=0$, and the second one at $t=\tau$ ($\tau=250$ fs); the echo is observed at $t=2\tau$.

evaluate long range electrostatic forces.[10,11] The CHARMM 19 all-atom potential energy function was used[12] and the dielectric constant was $\varepsilon=1$.

The molecular dynamics simulation used to obtain Fig. 9 and Fig. 13 are identical to that described in Ref. 4. It was performed with the CHARMM program (version 22)[12] and the all-atom parameter set.[13] A distance-dependent dielectric factor was employed ($\varepsilon=r$). In the simulations all the interactions were included, i.e., no distance cutoff for non-bonded interactions was used, and the time step was equal to 0.5 fs.

III. TEMPERATURE QUENCH ECHOES IN THE HARMONIC APPROXIMATION

In this section, we relate the temperature echo, in the harmonic approximation, to the temperature correlation function. The derivation closely follows that in Refs. 3–7. By introducing the temperature–temperature correlation function a more systematic approach to the temperature response of the system is developed. We show how the echo temperature (i.e., the system temperature at the time of the echo) is related to the density of states and that in a harmonic system the density of states can be extracted from the depth of the echo.

The normal mode analysis for proteins, particularly suitable at low temperatures, assumes that the potential energy surface on which the atoms move can be approximated by a quadratic form. The normal modes can be determined through the calculation and diagonalization of the second derivative (Hessian) matrices of the potential energy with respect to mass weighted Cartesian or internal coordinates. This method has been successfully employed for proteins.[14–16] Although there are anharmonic contributions to the energy function, the harmonic approximation can still

give insights into protein motions. An alternative route to evaluate normal modes is through diagonalization of the force–force correlation matrix $F_{jk}=\langle f_j f_k \rangle$, of the velocity-velocity correlation matrix $V_{jk}=\langle v_j v_k \rangle$, or of the coordinate-coordinate correlation matrix $X_{jk}=\langle \Delta x_j \Delta x_k \rangle$, where j, k label the three Cartesian coordinates of all N particles, and the average here is over trajectories lasting a sufficient period of time.[17,18]

For a protein with N atoms, there are $3N-6$ internal normal modes after the six degrees of freedom which describe overall translation and rotation are removed. We denote the frequency of the αth mode by ω_α and the associated vibrational coordinate by q_α, where $\alpha=1,2,...,3N-6$. The vibrational modes are assumed to be in mass-weighted coordinates, such that the effective mass associated with each mode is unity.[19]

To derive the relationship between the quench echo effect and the temperature correlation function, we need to analyze how the kinetic energy, or temperature defined in Eq. (1), evolves before the first quench, between the first and the second quench, and after the second quench.

A. Before the first quench

Before the first quench, i.e., for $t<0$, the probability for the αth normal mode to have amplitude A_α is given by the Rayleigh distribution[20]

$$P(A_\alpha)=\frac{\omega_\alpha^2 A_\alpha}{k_B T_0}\exp\left(-\frac{\omega_\alpha^2 A_\alpha^2}{2k_B T_0}\right), \quad (3)$$

where T_0 is the equilibrium temperature of the system.

We define by θ_α the phase of the αth normal mode at $t=0$. The values of θ_α are random and, at thermal equilibrium, can be assumed to be evenly distributed in the interval $[0, 2\pi]$. The position of the αth normal mode at $t<0$ can be expressed as

$$q_\alpha^{(1)}(t)=A_\alpha \cos(\omega_\alpha t+\theta_\alpha) \quad (4)$$

with corresponding velocity

$$v_\alpha^{(1)}(t)=\frac{dq_\alpha^{(1)}(t)}{dt}=-A_\alpha \omega_\alpha \sin(\omega_\alpha t+\theta_\alpha). \quad (5)$$

Thus, one obtains for the total kinetic energy $E_k^{(1)}$ the correlation function

$$\langle E_k^{(1)}(t)E_k^{(1)}(0)\rangle_\theta=\left\langle\left(\sum_\alpha \frac{1}{2}\omega_\alpha^2 A_\alpha^2 \sin^2(\omega_\alpha t+\theta_\alpha)\right)\right.$$

$$\left.\times\left(\sum_\lambda \frac{1}{2}\omega_\lambda^2 A_\lambda^2 \sin^2\theta_\lambda\right)\right\rangle_\theta, \quad (6)$$

where the summation over α and λ is from 1 to $3N-6$ and $\langle...\rangle_\theta$ denotes the average over the random phases θ_α and θ_λ. Employing the averaging technique proposed by Rayleigh,[20,21] one exploits

$$\langle\exp[\pm i(\theta_\alpha+\theta_\lambda)]\rangle_\theta=0; \quad \langle\exp[\pm i(\theta_\alpha-\theta_\lambda)]\rangle_\theta=\delta_{\alpha\lambda}, \quad (7)$$

and obtains

$$\langle E_k^{(1)}(t) E_k^{(1)}(0) \rangle_\theta = \left(\sum_\alpha \frac{1}{4} \omega_\alpha^2 A_\alpha^2 \right)^2$$

$$+ \sum_\alpha \frac{1}{32} \omega_\alpha^4 A_\alpha^4 \cos(2\omega_\alpha t). \qquad (8)$$

It is easy to show

$$\langle E_k^{(1)}(t) \rangle_\theta = \left\langle \sum_\alpha \frac{1}{2} \omega_\alpha^2 A_\alpha^2 \sin^2(\omega_\alpha t + \theta_\alpha) \right\rangle_\theta$$

$$= \sum_\alpha \frac{1}{4} \omega_\alpha^2 A_\alpha^2. \qquad (9)$$

The harmonic equations derived above can be further simplified by considering the ensemble averages of the kinetic energy and of the temperature. At equilibrium one can assume equipartition among the modes, which means that the average kinetic energy in each mode is

$$\langle E_{k,\alpha}^{(1)}(t) \rangle_{A,\theta} = \langle \tfrac{1}{2} v_\alpha^{(1)}(t)^2 \rangle_{A,\theta} = \tfrac{1}{2} k_B \langle T \rangle, \qquad (10)$$

where $\langle \ldots \rangle_{A,\theta}$ is the ensemble average over oscillator amplitudes A_α [using Eq. (3)] and over the random phases θ_α. In the following equations we use the subscript Z to indicate an ensemble average over both A and θ, i.e., $\langle \ldots \rangle_Z = \langle \ldots \rangle_{A,\theta}$. For individual normal modes, we have

$$\langle A_\alpha^2 \omega_\alpha^2 \sin^2(\omega_\alpha t + \theta_\alpha) \rangle_Z = k_B \langle T(t) \rangle_Z. \qquad (11)$$

By taking the time average we obtain for each mode

$$\tfrac{1}{2} \omega_\alpha^2 \langle A_\alpha^2 \rangle_Z = k_B \langle T \rangle_{Z,t}. \qquad (12)$$

Defining the average equilibrium temperature $T_0 = \langle T \rangle_{Z,t}$, one can write

$$\langle \omega_\alpha^2 A_\alpha^2 \rangle_Z = \langle A_\alpha^{*2} \rangle_Z = 2k_B T_0, \qquad (13)$$

i.e., the ensemble average of the factor $\omega_\alpha^2 A_\alpha^2$ is a constant proportional to the equilibrium temperature T_0. For convenience, we rename this factor A_α^{*2}, and rewrite Eq. (9) as

$$\langle E_k^{(1)}(t) \rangle_Z = \left\langle \sum_\alpha \frac{1}{2} A_\alpha^{*2} \sin^2(\omega_\alpha t + \theta_\alpha) \right\rangle_Z$$

$$= \left\langle \sum_\alpha \frac{1}{4} A_\alpha^{*2} \right\rangle_Z = (3N-6) \tfrac{1}{2} k_B T_0, \qquad (14)$$

where in the last equality we used Eq. (13) to get the expected result.

The normalized temperature–temperature correlation function is defined by

$$C_{T,T}(t) = \frac{\langle T(t)T(0) \rangle - \langle T(t) \rangle^2}{\langle [T(t)]^2 \rangle - \langle T(t) \rangle^2}. \qquad (15)$$

$C_{T,T}(t)$ can be expressed by use of Eqs. (1), (8) and (9) as

$$C_{T,T}(t) = \frac{\langle E_k^{(1)}(t) E_k^{(1)}(0) \rangle - \langle E_k^{(1)}(t) \rangle^2}{\langle [E_k^{(1)}(t)]^2 \rangle - \langle E_k^{(1)}(t) \rangle^2}$$

$$= \frac{\langle \Sigma_\alpha A_\alpha^{*4} \cos(2\omega_\alpha t) \rangle}{\langle \Sigma_\alpha A_\alpha^{*4} \rangle}. \qquad (16)$$

It should be noted that, as written, Eq. (1) includes the overall translation and rotation while the normal mode kinetic energy does not. In the use of simulations to evaluate the correlation functions, it would be appropriate to do simulations for a system with no overall translation or rotation, as is commonly done for vacuum simulations. For proteins or peptides in solution, a correction needs to be made; for most cases, the difference between $3N$ and $3N-6$ degrees of freedom is negligible.

Using distribution Eq. (3) one obtains for the denominator in Eq. (16)

$$\left\langle \sum_\alpha A_\alpha^{*4} \right\rangle = 8(3N-6)(k_B T_0)^2. \qquad (17)$$

For each simulation trajectory, A_α is a fixed constant which depends on the initial velocity assignment. However, as shown in Ref. 22, the correlation function is almost identical for different trajectories. Thus, we assume that $C_{T,T}(t)$ calculated from a given trajectory represents the temperature-temperature correlation function evaluated from the average over many trajectories with an ensemble of A_α distributed according to Eq. (3). Consequently, we obtain

$$C_{T,T}(t) = \frac{\langle \Sigma_\alpha A_\alpha^{*4} \cos(2\omega_\alpha t) \rangle_A}{8(3N-6)(k_B T_0)^2} = \langle \cos(2\omega_\alpha t) \rangle_\alpha, \qquad (18)$$

where $\langle \ldots \rangle_A$ denotes the average over the amplitudes of the oscillators determined by use of Eq. (3), and $\langle \ldots \rangle_\alpha$ is an average over all the normal modes, i.e.,

$$\langle f(\omega_\alpha) \rangle_\alpha = \frac{1}{3N-6} \sum_\alpha f(\omega_\alpha) = \int_0^\infty d\omega \, D(\omega) f(\omega). \qquad (19)$$

$D(\omega)$ denotes the normalized density of states. We use relation Eqs. (18) and (19) below to derive a method for determining the density of states from the temperature quench echo.

The correlation function $C_{T,T}(t)$ could be evaluated from Eqs. (18) and (19) if the density of states $D(\omega)$ were known. Here we determine $C_{T,T}(t)$, according to Eq. (15) from molecular dynamics simulations, which do not necessarily satisfy the harmonic approximation. $C_{T,T}(t)$ was calculated from the 10 to 15 ps interval in the 15 ps simulation described in Section II. The result is shown in Fig. 2. By using a least-square fit, the correlation function can be matched to a single exponential decay

$$C_{T,T}(t) \approx e^{-t/\tau_0}, \quad \tau_0 = 2.47 \text{ fs.} \qquad (20)$$

However, as is evident from Fig. 2, the exponential decay used in Eq. (20) is very approximate. The correlation function $C_{T,T}(t)$ has a long-time oscillatory behavior, which contains essential information concerning the density of states.
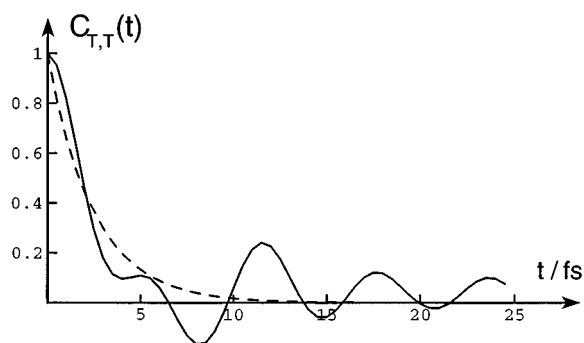
FIG. 2. The temperature correlation function. The solid line is calculated from a 5 ps simulation at $T_0 = 297.86$ K according to Eq. (15). Shown by a dashed line is a least-square fit to a single exponential decay $e^{-\tau/\tau_0}$ ($\tau_0 = 2.47$ fs).

B. After the first quench and before the second one

We now develop a description of the temperature echo in the framework of the harmonic approximation. At $t=0$, the velocities for all modes are set to zero. The amplitude for the αth normal mode is

$$A_\alpha^{(2)} = |q_\alpha^{(1)}(0)| = |A_\alpha \cos \theta_\alpha|. \tag{21}$$

The position and velocity for the α th normal mode at times $0 < t < \tau$ (i.e., after the first quench) can be expressed

$$q_\alpha^{(2)}(t) = \pm A_\alpha \cos \theta_\alpha \cos(\omega_\alpha t),$$
$$v_\alpha^{(2)}(t) = \mp A_\alpha \omega_\alpha \cos \theta_\alpha \sin(\omega_\alpha t). \tag{22}$$

The initial phases of all modes are $0, \pi$ due to the applied quench, resulting in the choice of $\pm$ signs. Accordingly, the total kinetic energy after the first quench and before the second quench is

$$\langle E_k^{(2)}(t) \rangle = \left\langle \sum_\alpha \frac{1}{2} A_\alpha^{*2} \cos^2 \theta_\alpha \sin^2(\omega_\alpha t) \right\rangle_Z$$
$$= \left\langle \sum_\alpha \frac{1}{8} A_\alpha^{*2} [1 - \cos(2\omega_\alpha t)] \right\rangle_Z$$
$$= \frac{3N-6}{8} \langle A_\alpha^{*2} \rangle_Z [1 - C_{T,T}(t)]. \tag{23}$$

From Eq. (13) and $\langle E_k^{(2)}(t) \rangle = (3N-6)/2\, k_B T^{(2)}(t)$, the temperature after the quench is given by

$$T^{(2)}(t) = \frac{T_0}{2} [1 - C_{T,T}(t)]. \tag{24}$$

This expression contains the correlation function, Eq. (15). One can see from Fig. 1 that the prediction given by Eq. (24), using a correlation function $C_{T,T}(t)$ determined from the simulation shown in Fig. 2, is in good agreement with the temperature response resulting from the molecular dynamics simulation. This is true in spite of the fact that Eq. (24) has been derived within the harmonic model and that the molecular dynamics simulations include the effect of anharmonic forces.

C. After the second quench

At $t=\tau$, the velocities for all the modes are set to zero again. The amplitude for the α th normal mode is

$$A_\alpha^{(3)} = |q_\alpha^{(2)}(\tau)| = |A_\alpha \cos \theta_\alpha \cos(\omega_\alpha \tau)|. \tag{25}$$

The velocity for the α th normal mode at $t \geq \tau$ is

$$v_\alpha^{(3)}(t) = \pm A_\alpha \omega_\alpha \cos \theta_\alpha \cos(\omega_\alpha \tau) \sin[\omega_\alpha(t-\tau)], \tag{26}$$

and the total kinetic energy is

$$E_k^{(3)}(t) = \sum_\alpha \frac{1}{2} \omega_\alpha^2 A_\alpha^2 \cos^2 \theta_\alpha \cos^2(\omega_\alpha \tau) \sin^2[\omega_\alpha(t-\tau)]. \tag{27}$$

Averaging over the initial ($t<0$) phase θ_α and the initial ($t<0$) amplitude A_α yields

$$\langle E_k^{(3)}(t) \rangle = \frac{3N-6}{16} \langle A_\alpha^{*2} \rangle_Z \left\{ 1 - \frac{1}{2} \langle \cos(2\omega_\alpha t) \rangle_\alpha - \frac{1}{2} \right.$$
$$\times \langle \cos[2\omega_\alpha(t-2\tau)] \rangle_\alpha + \langle \cos(2\omega_\alpha \tau) \rangle_\alpha$$
$$\left. - \langle \cos[2\omega_\alpha(t-\tau)] \rangle_\alpha \right\}. \tag{28}$$

According to Eqs. (13), (18), and $\langle E_k^{(3)}(t) \rangle = (3N-6)/2\, k_B T^{(3)}(t)$, the temperature response then obeys

$$T^{(3)}(t) = \frac{T_0}{4} [1 - C_{T,T}(t-\tau) + C_{T,T}(\tau)] - \frac{T_0}{8} [C_{T,T}(t) + C_{T,T}(|t-2\tau|)]. \tag{29}$$

For $t > \tau$, and $\tau \gg \tau_0$, where τ_0 is the relaxation time of the correlation function as given in Eq. (20), Eq. (29) can be simplified noting $C_{T,T}(\tau) \approx 0$ and $C_{T,T}(t) \approx 0$; we obtain, accordingly,

$$T^{(3)}(t) \approx \frac{T_0}{4} [1 - C_{T,T}(t-\tau)] - \frac{T_0}{8} C_{T,T}(|t-2\tau|). \tag{30}$$

For $\tau < t \ll 2\tau$ and $C_{T,T}(|t-2\tau|) \approx 0$, Eq. (30) reduces to

$$T^{(3)}(t) \approx \frac{T_0}{4} [1 - C_{T,T}(t-\tau)] \tag{31}$$

which expresses the temperature response in terms of the correlation function, Eq. (15). Figure 1 shows that Eq. (31), with $C_{T,T}(t)$ determined from the molecular dynamics simulation presented in Fig. 2, fits the simulation rather well.

At the time of the echo, when $t \approx 2\tau$ and $C_{T,T}(t-\tau) \approx 0$, Eq. (30) can be approximated

$$T^{(3)}(t) \approx \frac{T_0}{4} - \frac{T_0}{8} C_{T,T}(|t-2\tau|). \tag{32}$$

Equation (32) expresses the echo temperature in terms of the correlation function, Eq. (15). It predicts that in the limit of long times the depth of the echo should be constant and equal to $T_0/8$, i.e., at time $t \geq 2.47$ fs [see Eq. (20)], the echo depth is predicted to be independent of τ and, therefore, not related to the normal mode frequencies. However, the value $T_0/8$ is only an approximation since, as seen in Fig. 2, the fluctuations in the temperature–temperature correlation func-
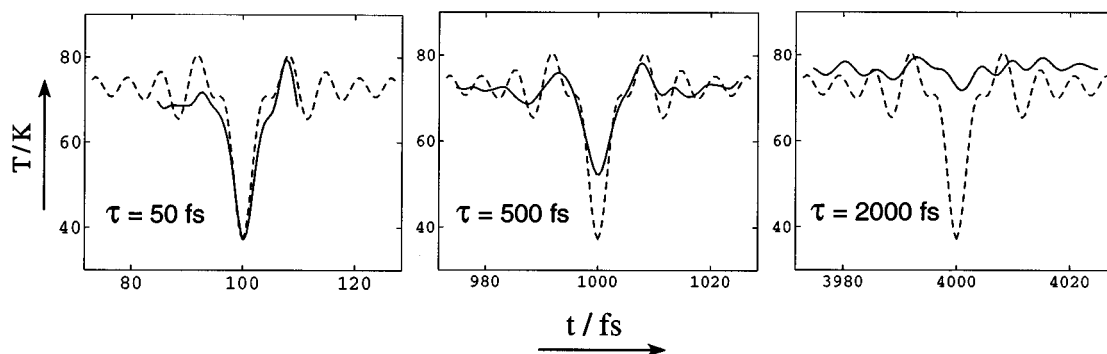
FIG. 3. Comparison of the echo depth for different τ. The solid lines represent simulations with the quench echo of temperature averaged over 6 runs for the protein BPTI; the dashed lines represent the prediction by the harmonic model, i.e., Eq. (32).

tion persist long after the initial exponential decay (with relaxation time of 2.47 fs) is over. These fluctuations carry important information concerning the density of states. In the next section we discuss the relationship between the echoes and the underlying vibrational density of states and demonstrate how the density of states can be extracted from the temperature echo depth in the harmonic limit.

In actual simulations of temperature echoes in proteins the echo-depth does not approach a constant value but rather decays to zero due to anharmonic effects, such as dephasing.[3,4,6,7] The dephasing contribution is analyzed in detail in Section V. For example, in Fig. 3 we see that while at $\tau=50$ fs the echo almost has the predicted depth of $T_0/8$ (37.2 K), but when τ becomes larger, the depth of the echo decreases. For $\tau=2$ ps, the echo almost disappears. Figure 3 also shows that the width of the echo is well described by the correlation function $C_{T,T}(|t-2\tau|)$.

D. Echoes after a sequence of three quenches

By quenching the system three times, namely at $t=0$, τ_1, τ_2, one can obtain additional echoes, as shown in Ref. 6. Using the technique described above, one can show that the temperature response after the third quench can be expressed as

$$T(t) = \frac{T_0}{8} \left[1 - C_{T,T}(t') \right] - \frac{T_0}{16} \left[C_{T,T}(|t'-\tau_1|) \right.$$

$$+ C_{T,T}(|t'-\tau_2|)] - \frac{T_0}{32} \left[C_{T,T}(|t'-\tau_1-\tau_2|) \right.$$

$$+ C_{T,T}(|t'-|\tau_2-\tau_1||)], \tag{33}$$

where $t' = t - \tau_1 - \tau_2$. From Eq. (33), one expects that there should be two echoes with depth of $T_0/16$ at $t' = \tau_1, \tau_2$, and two echoes with depth of $T_0/32$ at $t' = \tau_1 + \tau_2, |\tau_1-\tau_2|$. This behavior is demonstrated with the BPTI molecular dynamics simulations in Fig. 4.

IV. THE RELATIONSHIP BETWEEN QUENCH ECHOES AND THE DENSITY OF STATES

We return to the case of echoes resulting from the two quenches at $t=0,\tau$. If one plots the depth of the temperature

quench echo versus $2\pi/\tau$, one obtains the so-called echo-depth spectrum.[4] In Ref. 6 it was demonstrated that the echo depth spectrum for a Lennard-Jones glass has the same form as its density of states. Similarly, in Ref. 4 it was found that the echo-depth spectrum of BPTI is in agreement with the experimental density of states observed by inelastic neutron scattering,[23] and it was suggested that the double quench echoes can be used for estimating the density of states in general. The argument, which follows that of Nagel *et al.*,[6] was: When a system is quenched at time $t=0$, all oscillations of the system are forced to select a phase 0 or π. This is the same for the second quench at $t=\tau$. Thus, the second quench has no effect on motions of frequency π/τ or multiples thereof, since these motions are at their turning point when the second quench is applied. Then, at time 2τ, all the modes with frequencies of multiples of π/τ have vanishing kinetic
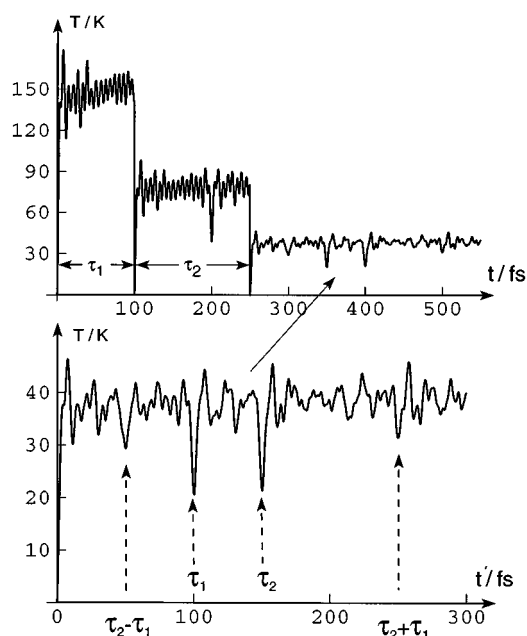
FIG. 4. The temperature versus time for BPTI quenched three times with $\tau_1=100$ fs, and $\tau_2=150$ fs. $t'=t-\tau_1-\tau_2$.

energy and, accordingly, contribute to the echo. It was thus concluded that if there are more modes with frequency $\omega = \pi/\tau$, a deeper echo is expected.

Such a description gives a heuristic picture of the temperature echo phenomenon. However, since there are a large number of normal modes for a Lennard-Jones glass or a protein, the modes with frequencies equal to multiples of π/τ make only a small contribution to the total kinetic energy. Also the absence of additional echoes at $t = 3\tau, 4\tau, \ldots$, besides the echo at $t = 2\tau$ in simulations of glasses as well as in ideal harmonic systems had not been understood. As shown in Section III for the harmonic model, the echo is a consequence of a coherent superposition of all vibrational modes and its depth does not directly mirror the density of states at the specific frequency $\omega = \pi/\tau$. In the following, we investigate how the double quench affects energies of different modes and derive the relationship between the echo-depth spectrum and the density of states.

A. The temperature quench as a filter of the energy spectrum

To study how temperature quenches affect the energy in different modes, we introduce an artificial ensemble of harmonic oscillators with frequencies ω_α, initial phases θ_α and mass weighted amplitudes A_α. The notations used here follow the ones in Section III. According to Eq. (25), the total energy (kinetic energy and potential energy) of the αth mode after two quenches is

$$E_{\text{tot}}(\omega_\alpha) = \tfrac{1}{2}\,\omega_\alpha^2 [A_\alpha^{(3)}]^2 = \tfrac{1}{2}\,\omega_\alpha^2 A_\alpha^2 \cos^2\theta_\alpha \cos^2(\omega_\alpha\tau);$$
(34)

and from Eq. (27), the kinetic energy of the αth mode at $t = 2\tau$ is

$$E_K(\omega_\alpha)\big|_{t=2\tau} = \tfrac{1}{2}\,\omega_\alpha^2 A_\alpha^2 \cos^2\theta_\alpha \cos^2(\omega_\alpha\tau)\sin^2(\omega_\alpha\tau).$$
(35)

We consider a system with 4000 normal modes with a density of states $D(\omega) \propto \sqrt{\omega}$ with a cutoff of 10, i.e., $0 < \omega < 10$. The frequencies are randomized to avoid possible resonance effects in the system. For this purpose, we generate random numbers η_α evenly distributed in the interval $[0,1]$. We attribute to each mode α, $\alpha = 1,2,\ldots,4000$, the frequency $\omega_\alpha = 10\eta_\alpha^{2/3}$. One can show

$$D(\omega)\,d\omega \propto D[\eta(\omega)]\,d\eta(\omega)$$

$$= D(\eta)\,\frac{d\eta(\omega)}{d\omega}\,d\omega \propto \sqrt{\omega}\,d\omega, \quad 0 < \omega < 10. \quad (36)$$

To further simplify the calculation in Eqs. (34) and (35), we assume

$$y_\alpha = \sqrt{\omega_\alpha^2 A_\alpha^2 / k_B}.$$
(37)

One then obtains the distribution function for y_α:

$$P(y_\alpha) = \frac{y_\alpha}{T_0}\exp\!\left(-\frac{y_\alpha^2}{2T_0}\right)$$
(38)
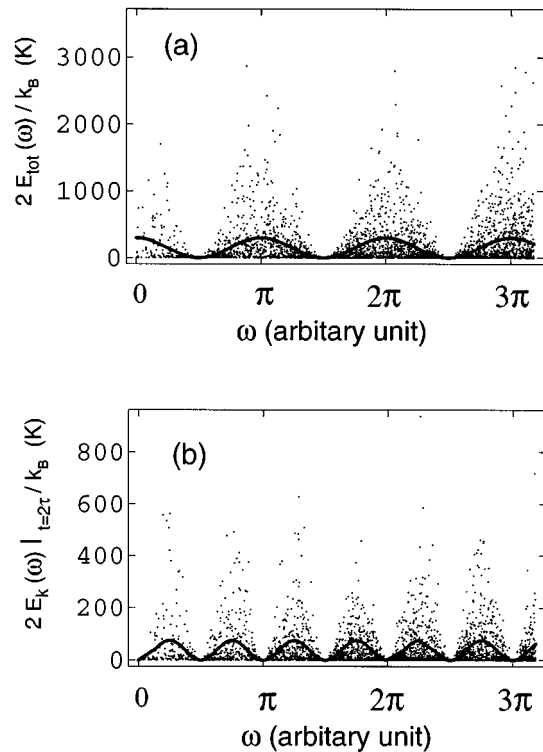
FIG. 5. Energy spectrum of a harmonic system after double quenches. (a) the total energy of each mode after two quenches. (b) the kinetic energy distribution at $t = 2\tau$. The dots in (a) and (b) represent energies according to Eqs. (39) and (41) by using random amplitudes y_α satisfying distribution (38) and random phases θ_α evenly distributed in the range of $[0,2\pi]$. The solid lines represent the averaged energies as given by Eqs. (40) and (42).

which is transformed from the distribution given by Eq. (3). We introduce 4000 random numbers for the y_α, distributed in accord with Eq. (38). Finally we generate random phases θ_α evenly distributed in the range of $[0,2\pi]$.

After a sequence of two quenches the total energy $E_{\text{tot}}(\omega_\alpha)$ (kinetic plus potential energy) in mode α obeys

$$2E_{\text{tot}}(\omega_\alpha)/k_B = y_\alpha^2 \cos^2\theta_\alpha \cos^2(\omega_\alpha\tau),$$
(39)

an expression which can be obtained from Eq. (34) after substituting for y_α as defined above. Note, that by dividing the energy by k_B we are evaluating it on a temperature scale. By averaging over the phases and amplitudes, the average total energy of the αth mode satisfies

$$\langle 2E_{\text{tot}}(\omega_\alpha)/k_B\rangle = T_0 \cos^2(\omega_\alpha\tau).$$
(40)

Similarly, at $t = 2\tau$, from Eq. (35) one obtains

$$2E_K(\omega_\alpha)\big|_{t=2\tau}/k_B = y_\alpha^2 \cos^2\theta_\alpha \cos^2(\omega_\alpha\tau)\sin^2(\omega_\alpha\tau),$$
(41)

and the effective temperature $T(\omega_\alpha)\big|_{t=2\tau}$ of the αth mode at $t = 2\tau$, through the relationship $\langle E_K(\omega_\alpha)\rangle = \tfrac{1}{2}k_B T(\omega_\alpha)$, is

$$T(\omega_\alpha)\big|_{t=2\tau} = \langle 2E_K(\omega_\alpha)\big|_{t=2\tau}/k_B\rangle$$

$$= T_0 \cos^2(\omega_\alpha\tau)\sin^2(\omega_\alpha\tau).$$
(42)

The results obtained from Eqs. (39)–(42) at 300 K are shown in Fig. 5. Figure 5(a) shows that the double quench has no effect on energies with frequencies of multiples of π/τ
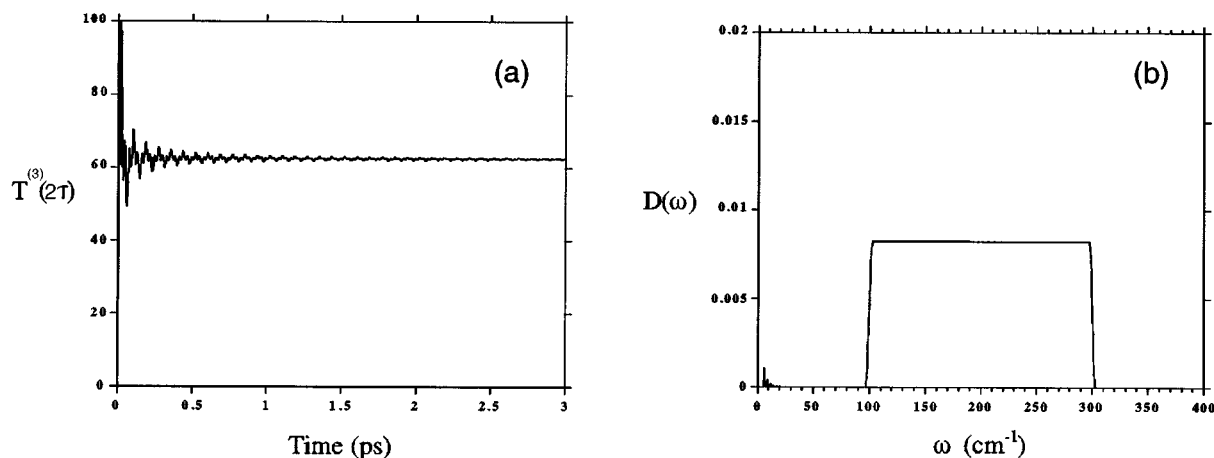
FIG. 6. A harmonic model with a block-shaped density of states $D(\omega)$ between 100 and 300 cm^{-1}: (a) the echo temperature $T^{(3)}(2\tau)$ as a function of τ; (b) the cosine transform of (a) showing that the density of states $D(\omega)$ is recovered from the temperature echo experiment.

while it filters out completely the modes with frequencies $n\pi/\tau + \pi/2$, where $n=0,1,2,...$ However, the range of frequencies in the neighborhood of multiples of π/τ that still contribute to the kinetic energy is rather broad. At $t=2\tau$, there is a kinetic energy filter $\sin^2(\omega_\alpha\tau)$ acting on the total energy spectrum shown in Fig. 5(b). The modes with frequencies of multiples of π/τ and a width of $\pi/4\tau$ contribute little kinetic energy so that an echo occurs. This means that the double quench does not fully isolate certain modes in accord with the heuristic picture given above. However, as we show in the following section, the density of states can be extracted from the echo depth spectrum.

B. Detailed time dependence of the echo temperature

Equation (32) predicts that in the limit $\tau \gg \tau_0$, the echo depth is independent of τ and of the distribution of normal mode frequencies. We show below that for short τ the echo depth is related to the density of states $D(\omega)$ in a simple way. For harmonic systems the relationship derived can be used to extract the density of states.

According to Eq. (29), the average system temperature after the second quench at $t=2\tau$ is

$$T^{(3)}(2\tau) = \frac{T_0}{8}[1 - C_{T,T}(2\tau)]. \qquad (43)$$

Based on Eqs. (18) and (19), Eq. (43) can be rewritten in terms of the normalized density of states $D(\omega)$

$$T^{(3)}(2\tau) = \frac{T_0}{8}\int_0^\infty d\omega\, D(\omega)[1 - \cos(4\omega_\alpha\tau)], \qquad (44)$$

where we have replaced the discrete summation over the $(3N-6)$ modes by an integral over $D(\omega)$. For proteins this is a very good approximation over the frequency range of primary interest $(0<\omega<500$ cm$^{-1})$.[15]

Thus, the ensemble average of the echo temperature is related to the density of states $D(\omega)$ by a cosine transform. The same cosine transform relation holds for simple linear

functions of the echo temperature, such as the echo-depth [which equals the constant asymptotic value $T_0/4$ minus the average echo temperature given in Eq. (44)].

Figure 6 demonstrates, for a harmonic model system, that the density of states can be obtained from the echo temperatures. Five hundred equally spaced modes, between 100 and 300 cm^{-1}, were generated to form a block-shaped density of states. To calculate the ensemble average of the echo-temperature $T^{(3)}(2\tau)$ as a function of τ, we use this density of states with the following equation derived from Eq. (27):

$$T^{(3)}(2\tau) = \frac{1}{(3N-6)}$$

$$\times\left\langle \sum_\alpha A_\alpha'^2 \cos^2(\omega_\alpha\tau)\, \sin^2[\omega_\alpha\tau]\right\rangle_Z, \qquad (45)$$

where $\langle A_\alpha'^2\rangle_Z = \langle A_\alpha^{*2}/(2k_B)\rangle_Z = \langle\omega_\alpha^2 A_\alpha^2\rangle_Z\langle\cos^2\theta_\alpha\rangle_Z/k_B$. Since the ensemble average of the factor $A_\alpha'^2$ is a constant, independent of the mode, it was set equal for all modes (a value of unity was used for simplicity). Figure 6(b) shows the cosine transform of $T^{(3)}(2\tau)$ for this system. It is clear that the density of states is recovered from the echo temperatures.

In another, more realistic example, we randomly generated 10 000 modes corresponding to a density of states $D(\omega) \propto \sqrt{\omega}$ with a cutoff, i.e., $0<\omega<10$, with the method as described in Section IV A. We then used this density of states to calculate the response of the model system to temperature quenches. Figure 7, which shows the temperature as a function of time for four different τ values, demonstrates the relationship between the echo depth and the time interval τ. For large τ ($\tau=1$ and $\tau=100$), the depth of the echo is a constant $T_0/2$ as shown in Eq. (32). For small τ ($\tau=0.2$), the echo at time $t\approx 2\tau$, is not discernible since it is completely masked by the large temperature fluctuations which characterize the relaxation process that follows every quench [in this case, the second quench described by Eq. (31)]. Moreover, the asymptotic value of temperature at $t\gg 2\tau$ is
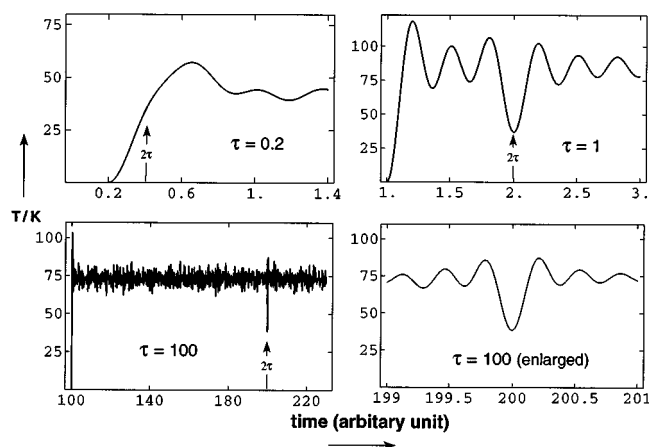
FIG. 7. A harmonic model with a density of states randomly generated to mimic $D(\omega) \propto \sqrt{\omega}$ with a cutoff, i.e., $0 < \omega < 10$. The figures give the temperature trajectories after the second quench for three different τ values.

$T_0/4[1 + C_{T,T}(\tau)]$, which can be significantly different from $T_0/4$ (the value in the limit of long times) due to large contribution of $C_{T,T}(\tau)$ in Eq. (29) when τ is small. Thus, the value of $T(2\tau)$ does change as a function of τ so that from a collection of such calculations one can generate the ''echotemperature spectrum'' and then perform a cosine transform of the result. Figure 8 compares the normalized result of this cosine transform to the actual normalized density of states used in the model simulation generated by the above procedure. The cosine transform was performed using Filon's formula with window smoothing.[24] One clearly sees that the density of states $D(\omega)$ calculated by transforming the echotemperatures is in very good agreement with the actual $D(\omega)$, including its deviations from the overall ($\sqrt{\omega}$) behavior.
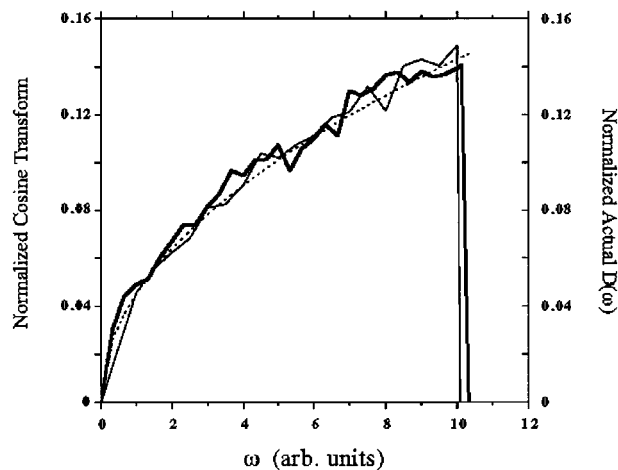
FIG. 8. The same harmonic model as in Fig. 7. Shown are the actual density of states used (thin line) and the function obtained by taking a cosine transform of the echo-temperatures $T^{(3)}(2\tau)$ (heavy line). Both functions were normalized to unity. One sees that the density of states $D(\omega)$ is recovered from the temperature quench echo experiment. The dashed line represents a $\sqrt{\omega}$ function.

C. Temperature quenches and the velocity autocorrelation function

Another way to obtain the density of states from the temperature quench experiment was suggested earlier by Grest *et al.*[7] In this method the response of the system to a single temperature perturbation was studied. Using Eqs. (23), (18) and (19) the temperature response to a single quench in terms of the normalized density of states $D(\omega)$ can be written

$$T^{(2)}(t) = \frac{T_0}{2} \int_0^\infty d\omega \, D(\omega)[1 - \cos(2\omega_\alpha t)], \qquad (46)$$

which means that the temperature response to a single quench is related to the density of states $D(\omega)$ by a cosine transform with the argument $2\omega t$.

Following Grest *et al.*[7] we define the function

$$K(t) = \left\langle 1 - \frac{T^{(2)}(t)}{T_\infty} \right\rangle_Z \qquad (47)$$

which has limits similar to those of a normalized correlation function. Here T_∞ is the asymptotic value of $T^{(2)}(t)$, i.e., $T_\infty = T_0/2$. By substituting Eq. (46) into Eq. (47), and noting that the integral over the normalized density of states is one, we obtain

$$K(t) = \int_0^\infty d\omega \, D(\omega) \, \cos(2\omega_\alpha \tau). \qquad (48)$$

Comparison with Eq. (18) shows that in harmonic systems $K(t)$ and $C_{T,T}(t)$ are identical; i.e.,

$$K(t) = \langle \cos(2\omega_\alpha t) \rangle_\alpha = C_{T,T}(t). \qquad (49)$$

The detailed relationship between the quench echo effect and the temperature correlation function was not studied in earlier work and no physical interpretation of $K(t)$ was given.

In the harmonic approximation, it also can be shown, using the same techniques as in Eqs. (3)–(19), that the velocity-velocity autocorrelation function can be expressed

$$C_{v,v}(t) = \frac{\langle v_\alpha(0)v_\alpha(t) \rangle_\alpha}{\langle v_\alpha^2 \rangle_\alpha} = \langle \cos(\omega_\alpha t) \rangle_\alpha = C_{T,T}(t/2).$$
$$(50)$$

From Eqs. (49) and (50) we see that for harmonic systems the temperature response function $K(t)$ and the temperature correlation function $C_{T,T}(t)$ are equal to the velocity autocorrelation function of the system if one replaces the argument t of $K(t)$ by $t/2$ where t is the argument of the velocity autocorrelation function $C_{v,v}(t)$.

Since Eq. (50) assumes the harmonic approximation, it is valid only at low temperatures, as has been demonstrated by Grest *et al.* for a Lennard-Jones glass.[7] At higher temperatures anharmonicities become significant and cause both $K(t)$ and $C_{T,T}(t)$ to deviate from the velocity autocorrelation function [not necessarily in the same way, since for anharmonic systems, Eq. (49) does not hold and these two functions are no longer identical].

Figure 9 shows the temperature response function $K(t)$ obtained from simulations in which an equilibrated BPTI molecule was subjected to a single quench and then allowed
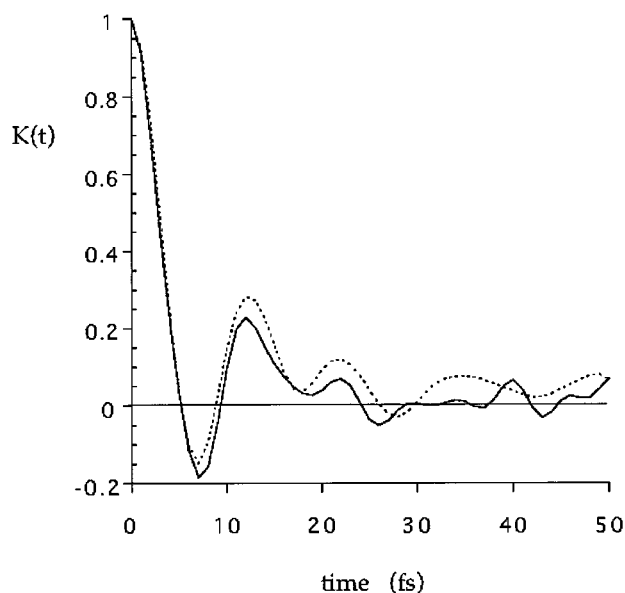
FIG. 9. The temperature response function $K(t)$ of an equilibrated BPTI molecule subjected to a single quench and then allowed to relax without further perturbation. Shown is the response at two different asymptotic temperatures, 66 K (solid line) and 140 K (dotted line), each averaged over three initial conditions.

FIG. 10. Comparison of quench echoes with $\tau=250$ fs resulting from simulations carried out with different numerical accuracies. The dotted line represents a simulation performed using the fast multipole approximation to calculate Coulomb interactions and a timestep of 0.5 fs. The solid line represents a simulation performed with a time step of 0.25 fs and without any approximation for calculating Coulomb interactions.

to relax without further perturbation. Shown is the response at two different asymptotic temperatures, 66 K and 140 K, each averaged over three initial conditions. Although the difference between the two curves, corresponding to two relatively low temperatures, is not very large, one clearly sees that $K(t)$ is temperature dependent. A comparison with Fig. 2, which depicts $C_{T,T}(t)$ at 297 K, further highlights the temperature dependence of these two functions.

Figure 9 is also qualitatively similar to "standard" velocity autocorrelation functions calculated directly from molecular dynamics simulations (cf., for example Ref. 25). However, there is a significant difference between these two functions. While the temperature quench response function $K(t)$, and $C_{T,T}(t)$, are already averaged over all atoms and modes of the system the standard velocity autocorrelation function is usually calculated for individual atom and subsequently averaged over the system. Thus, the temperature echo approach obtains the results for the entire system in a more direct manner.

In the Appendix, we show in more detail for a model system why the temperature correlation function is more appropriate for studying quench echoes.

V. EFFECTS DUE TO ANHARMONIC INTERACTIONS

The reason why the depth of the echo is not as deep as predicted by the harmonic model has been pointed out in Refs. 4 and 6 namely, that the system is not purely harmonic.[26] There exist important anharmonic contributions that arise from torsional, electrostatic and van der Waals interactions that contribute to the potential in proteins. Hence, the derivation in Section III, based upon the harmonic assumption, is not perfectly valid. It is true also that the errors accumulated in the numerical integrations of simulations
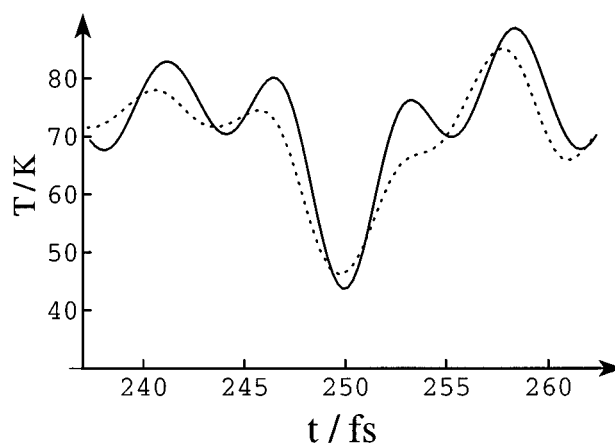
could make trajectories deviate from the harmonic behavior. We compared quench echoes with $\tau=250$ fs obtained from simulations carried out with different numerical precision. One simulation was performed using the fast multipole approximation to calculate Coulomb interactions with a timestep of 0.5 fs. This method has an inherent inaccuracy in evaluating the Coulomb forces as described in Ref. 11. Another simulation was performed with a time step of 0.25 fs and without any approximation for calculating Coulomb interactions, and thus with a higher numerical accuracy. The latter simulation (i.e., the more accurate simulation), shows a deeper and more symmetrical echo, and in this respect, yields an echo closer to what is predicted by the harmonic model (see Fig. 10). This suggests that the temperature echo results are sensitive to the accuracy of the force evaluation and numerical integration in molecular dynamics simulations.

To describe analytically how anharmonic interactions affect the echo depth, we consider a heuristic model which introduces the dephasing of the normal mode motions as a function of time. The velocity or coordinate of the αth normal mode, in the harmonic approximation, is described by $A_\alpha \sin(\omega_\alpha t)$. This harmonic motion interacts with other normal modes due to the anharmonic terms in the potential. Since the number of interactions are very large, we can consider such interactions as stochastic. The amplitude A_α of the αth oscillator obeys the distribution function of Eq. (3) and has been averaged in the derivation in Section III, such that the fluctuation of A_α does not affect the depth of the echo significantly. However, the anharmonic interaction can cause the trajectory to become dephased, i.e., the trajectory can be assumed to have a random phase δ_α in addition to the original phase term. Hence, the motion can be described by $A_\alpha \sin(\omega_\alpha t + \delta_\alpha)$. We demonstrate that such dephasing can explain the decrease of the echo depth.

We assume that at $t=0$, the phase δ_α of the αth mode is 0. With increasing time, anharmonic interactions add random
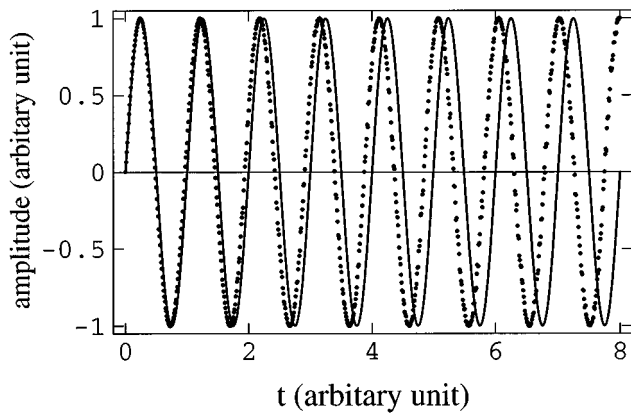
FIG. 11. A demonstration of dephasing. The solid line represents a harmonic motion with the form $\sin(\omega_\alpha t)$. The dots represent a dephased trajectory described by $\sin(\omega_\alpha t + \delta_\alpha)$ when δ_α is simulated by a so-called Wiener process which obeys Eq. (53). At $t=0$, the random phase δ_α is 0.

values to δ_α (see the demonstration in Fig. 11). The cumulative effect of such a process may be described by the Einstein diffusion equation

$$\partial_t P(\delta_\alpha, t) = D_\alpha \partial_{\delta_\alpha}^2 P(\delta_\alpha, t); \quad P(\delta_\alpha, 0) = \delta(\delta_\alpha), \quad (51)$$

where $P(\delta_\alpha, t)$ is the probability of having a random phase δ_α at time t. D_α in Eq. (51) is a diffusion constant and can be related to a temperature-independent constant, γ_α, the mobility constant, through[27]

$$D_\alpha = \gamma_\alpha k_B T. \quad (52)$$

The solution of Eq. (51) is the standard one-dimensional diffusion probability distribution

$$P(\delta_\alpha, t) = \frac{1}{\sqrt{4\pi\gamma_\alpha k_B T t}} \exp\left(-\frac{\delta_\alpha^2}{4\gamma_\alpha k_B T t}\right). \quad (53)$$

Accordingly, Eq.(27) can be written

$$\langle E_k^{(3)}(t) \rangle = \left\langle \left\langle \left\langle \left\langle \sum_\alpha \frac{1}{2} \omega_\alpha^2 A_\alpha^2 \cos^2 \theta_\alpha \cos^2[\omega_\alpha \tau \right.\right.\right.\right.$$
$$\left.+ \delta_{\alpha,1}(\tau)] \sin^2[\omega_\alpha(t-\tau) \right.$$
$$\left.\left.\left.\left.+ \delta_{\alpha,2}(t-\tau)] \right\rangle_\theta \right\rangle_A \right\rangle_{\delta_{\alpha,1}} \right\rangle_{\delta_{\alpha,2}}, \quad (54)$$

where $\delta_{\alpha,1}(t)$ is the random phase attached after the first quench and before the second one; $\delta_{\alpha,2}(t)$ is the random phase attached after the second quench, and $\langle ... \rangle_{\delta_{\alpha,i}}$ is defined as

$$\langle f(\delta_{\alpha,i}, t) \rangle_{\delta_{\alpha,i}} = \int_{-\infty}^{\infty} d\,\delta_{\alpha,i} P(\delta_{\alpha,i}, t) f(\delta_{\alpha,i}, t). \quad (55)$$

The depth of the echo can be expressed as

$$\Delta T(2\tau) = T^{(3)}(t \to \infty) - T^{(3)}(2\tau), \quad (56)$$

or

$$\Delta T(2\tau) = \left\langle \left\langle \left\langle \left\langle \sum_\alpha \frac{1}{2} \omega_\alpha^2 A_\alpha^2 \cos^2 \theta_\alpha \cos^2[\omega_\alpha \tau \right.\right.\right.\right.$$
$$\left.+ \delta_{\alpha,1}(\tau)] \left\{ \frac{1}{2} - \sin^2[\omega_\alpha \tau \right.\right.$$
$$\left.\left.\left.\left.\left.+ \delta_{\alpha,2}(\tau)] \right\} \right\rangle_\theta \right\rangle_A \right\rangle_{\delta_{\alpha,1}} \right\rangle_{\delta_{\alpha,2}}$$

$$= \frac{T_0}{8} \{ \langle \langle \langle \cos[-2\delta_{\alpha,1}(\tau) + 2\delta_{\alpha,2}(\tau)] \rangle_{\delta_{\alpha,1}} \rangle_{\delta_{\alpha,2}} \rangle_\alpha$$
$$+ \langle \langle \cos[2\omega_\alpha \tau + 2\delta_{\alpha,2}(\tau)] \rangle_{\delta_{\alpha,2}} \rangle_\alpha$$
$$+ \langle \langle \langle \cos[4\omega_\alpha \tau + 2\delta_{\alpha,1}(\tau)$$
$$+ 2\delta_{\alpha,2}(\tau)] \rangle_{\delta_{\alpha,1}} \rangle_{\delta_{\alpha,2}} \rangle_\alpha \}. \quad (57)$$

For large τ the last two terms of the r.h.s. are very small and the depth of the echo at $t=2\tau$ is essentially

$$\Delta T(\tau) = \left(\frac{T_0}{8}\right) \langle \langle \langle \cos[-2\delta_{\alpha,1}(\tau) + 2\delta_{\alpha,2}(\tau)] \rangle_{\delta_{\alpha,1}} \rangle_{\delta_{\alpha,2}} \rangle_\alpha, \quad (58)$$

where $\langle ... \rangle_\alpha$ has been defined in Eq. (19).

The distribution for $\delta_{\alpha,1}(\tau)$ is

$$P[\delta_{\alpha,1}(\tau), \tau] = \frac{1}{\sqrt{2\pi\gamma_\alpha k_B T_0 \tau}} \exp\left(-\frac{\delta_{\alpha,1}^2(\tau)}{2\gamma_\alpha k_B T_0 \tau}\right); \quad (59)$$

and for $\delta_{\alpha,2}(\tau)$ is

$$P[\delta_{\alpha,2}(\tau), \tau] = \frac{1}{\sqrt{\pi\gamma_\alpha k_B T_0 \tau}} \exp\left(-\frac{\delta_{\alpha,2}^2(\tau)}{\gamma_\alpha k_B T_0 \tau}\right). \quad (60)$$

The difference between Eqs. (59) and (60) is due to the different reference temperatures, $T_0/2$ for $\delta_{\alpha,1}(\tau)$ and $T_0/4$ for $\delta_{\alpha,2}(\tau)$. Let

$$\xi_\alpha = -\delta_{\alpha,1}(\tau) + \delta_{\alpha,2}(\tau). \quad (61)$$

Since $\delta_{\alpha,1}(\tau)$ and $\delta_{\alpha,2}(\tau)$ are independent Gaussian random variables, the distribution for ξ_α at τ is again Gaussian, namely,

$$P(\xi_\alpha, \tau) = \frac{1}{\sqrt{3\pi\gamma_\alpha k_B T_0 \tau}} \exp\left(-\frac{\xi_\alpha^2}{3\gamma_\alpha k_B T_0 \tau}\right). \quad (62)$$

Hence, one obtains

$$\Delta T(\tau) = \left(\frac{T_0}{8}\right) \left\langle \int_{-\infty}^{\infty} d\xi_\alpha \cos(2\xi_\alpha) \frac{1}{\sqrt{3\pi\gamma_\alpha k_B T_0 \tau}} \right.$$
$$\left. \times \exp\left(-\frac{\xi_\alpha^2}{3\gamma_\alpha k_B T_0 \tau}\right) \right\rangle_\alpha$$

$$= \left(\frac{T_0}{8}\right) \langle \exp(-3\gamma_\alpha k_B T_0 \tau) \rangle_\alpha. \quad (63)$$

In case γ_α is the same constant γ_0 for all modes, we have

$$\Delta T(\tau) = \frac{T_0}{8} \exp(-3\gamma_0 k_B T_0 \tau). \quad (64)$$
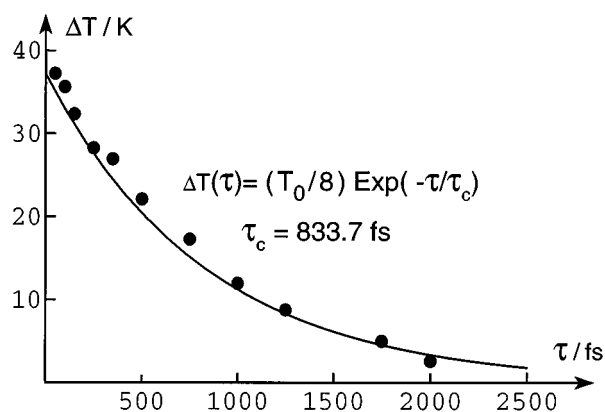
FIG. 12. Comparison of the echo depth resulting from simulations and predicted by Eq. (64). The simulation results were averaged over six runs for BPTI. The τ_c value was chosen through a least-square fit.

In Fig. 12, we compare the echo depth resulting from simulations and predicted by Eq. (64). One can see that Eq. (64) with $\tau_c = 1/(3\gamma_0 k_B T_0) = 883.7$ fs fits the simulations very well; the value of τ_c was obtained from a least-square fit to the results.

In Fig. 13, we consider the τ-dependence of the echo depth. We have carried out temperature quenches as described above for many different τ values in the range $0 < \tau \leqslant 1.5$ ps with interval of 25 fs. For each τ value, we carried out quenches with three different initial conformations and then determined the average echo depth. Figure 13 reveals that although the result can be fit to an exponential function (as in Fig. 12, only in this case we obtain a slightly different $\tau_c = 846.7$ fs) the exponential fit is only an approximate description. The actual echo-depth temperature fluctuates around the exponential fit of Eq. (64). Clearly, part of the observed fluctuations arise from insufficient averaging, but the deviation from Eq. (64) is also due to the simplifying
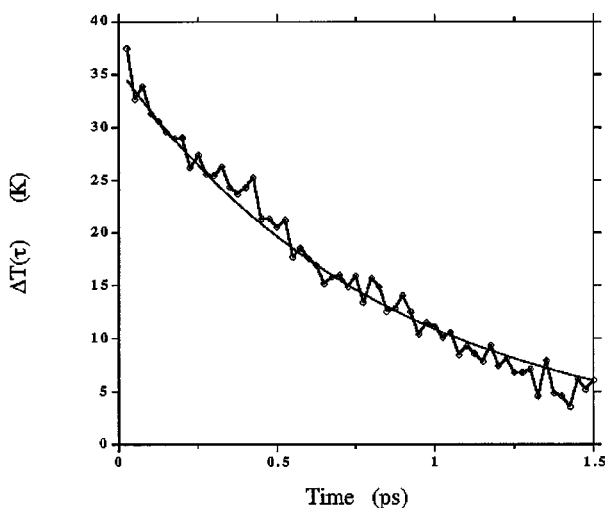
FIG. 13. The echo depth as a function of time, resulting from simulations for BPTI averaged over 3 different initial conditions (heavy line). The τ values corresponding to the data points are separated by 25 fs. The thin line is an exponential fit similar to that in Fig. 12 (here $\tau_c = 846.7$ fs).

assumptions used in deriving Eqs. (58)–(64), particularly due to the neglect of the dependence on the density of states.

VI. DISCUSSION AND CONCLUSIONS

We have used the temperature–temperature correlation function to analyze temperature echoes in a harmonic system and demonstrated analytically and numerically that the double quench echoes can be used to obtain the density of states $D(\omega)$. However, in cases where anharmonicities are significant (this is likely to be true for most biopolymer systems except at very low temperatures), modal dephasing dominates the decay of the echoes. If one quenches the system many times with the same time intervals τ, all the modes are gradually drained of energy except those with frequencies at multiples of π/τ and the depth of the echo is related to the density of state $D(\pi/\tau)$ even if anharmonic effects are present. This method to measure $D(\omega)$ was suggested in Refs. 3 and 6. From the present analysis it appears that the method would have relatively large errors. This is due to the fact that the anharmonic effects will accumulate over the multiple quenches and that modes with frequencies at multiples of π/τ will contribute to the echo. A detailed discussion of these phenomena will be given elsewhere.[28]

As already observed in Ref. 4, it is of interest that a protein exhibits echoes at 300 K for 1 ps or longer. A temperature of 300 K is considerably above the "glass transition" temperature for a protein, which is in the neighborhood of 220 K; the transition is present in vacuum simulations of the type used in this work.[29] Thus, dephasing of the normal modes is a relatively slow process despite the presence of anharmonic contributions to the potential.

In this paper we discussed only the original type of temperature quench echoes. Other types of perturbation schemes, such as the cool-heat-cool temperature pulse sequence[4,28] and the velocity reassignment echo[30] are discussed elsewhere. In all cases one is studying the response of the system to velocity perturbations which involve a coherent excitation of all protein modes.

From the present analysis it appears that the temperature echoes may be useful for examining the anharmonic properties in protein systems. The results indicate that the decay of echo depth versus time can provide a measure of the time scale of the vibrational decoherence.

There remain many interesting questions regarding temperature echoes. For example, the simulations revealed that the friction describing the decoherence of the normal modes is temperature-dependent.[30] This temperature dependence may shed some light on dynamic properties of proteins, e.g., their relationship to glasses. Temperature echoes can also be applied locally. For example, it may be possible to probe certain functional groups inside biomolecules, e.g., a particular residue, by perturbing only the atomic velocities involving these groups and measuring the echo of the local temperature response. The procedure for temperature echoes can also be generalized to dynamic variables other than temperature; an example would be to follow the protein dipole moment after electric field jumps.

ACKNOWLEDGMENTS

APPENDIX: THE TEMPERATURE CORRELATION FUNCTION IN THE FRAMEWORK OF LINEAR RESPONSE THEORY

We employed in our description above the temperature correlation function rather than the velocity correlation function, since in linear response theory, the response of the system to a brief temperature pulse is related to the temperature-temperature correlation function. To demonstrate this relationship, consider a single particle described by the Langevin equation

$$m\ddot{x} = f(x) - \gamma\dot{x} + \sigma\xi. \tag{A1}$$

The response function is defined as[31]

$$R_{E_k,l}(t) = \langle E_k(t)A(0)\rangle, \tag{A2}$$

where

$$A = p_0^{-1}(x,v)lp_0(x,v). \tag{A3}$$

Here $p_0(x,v)$ is the stationary position-velocity distribution of the particle and l is an operator which describes a perturbation applied at $t=0$. For $p_0(x,v) \sim \exp(-mv^2/(2k_B T_0))$ and $l = \partial_v^2$ holds

$$A = -\frac{m}{k_B T_0} + \frac{2m}{(k_B T_0)^2}\left(\frac{1}{2}mv^2\right). \tag{A4}$$

Hence, one obtains

$$R_{E_k,l}(t) = -\frac{m}{k_B T_0}\langle E_k(t)\rangle + \frac{2m}{(k_B T_0)^2}\langle E_k(t)E_k(0)\rangle$$

$$= -\frac{m}{2} + \frac{2m}{(k_B T_0)^2}\langle E_k(t)E_k(0)\rangle. \tag{A5}$$

According to Eq. (16) and Eq. (17), follows within the harmonic approximation

$$C_{T,T}(t) = \frac{\langle E_k(t)E_k(0)\rangle}{8(k_B T_0)^2} - \frac{1}{32}. \tag{A6}$$

Comparing Eq. (A5) and Eq. (A6), one concludes

$$R_{E_k,l}(t) = 16m C_{T,T}(t). \tag{A7}$$

The operator l describes a perturbation $\delta(t)\epsilon\partial_v^2$, which is added to the Fokker–Planck operator corresponding to the Langevin equation Eq. (A1), namely, to

$$\mathscr{L}_0(\mathbf{x},\mathbf{v}) = \frac{k_B T_0 \gamma}{m^2}\partial_v^2 + \frac{1}{m}\partial_v[\gamma v - f(x)] - \partial_x v. \tag{A8}$$

Obviously, the additive perturbation $\delta(t)\epsilon\partial_v^2$ in Eq. (A8) corresponds to a sudden temperature pulse $\Delta T\delta(t)$ in the system, where

$$\Delta T = \frac{m^2\epsilon}{k_B\gamma}. \tag{A9}$$

Hence, we have demonstrated that the response of the system to a temperature pulse $\Delta T\delta(t)$, described by $R_{T,l}(t)$, is equal to the temperature–temperature correlation function $C_{T,T}(t)$.

[1] J. A. McCammon and S. C. Harvey, *Dynamics of Proteins and Nucleic Acids* (Cambridge University Press, Cambridge, 1987).

[2] C. L. Brooks III, M. Karplus, and B. Pettitt, *Proteins*; *Advances in Chemical Physics Vol. LXXI* (Wiley, New York, NY, 1988).

[3] G. S. Grest, S. R. Nagel, and A. Rahman, Solid State Commun. **36**, 875 (1980).

[4] O. M. Becker and M. Karplus, Phys. Rev. Lett. **70**, 3514 (1993).

[5] S. R. Nagel, A. Rahman, and G. S. Grest, Phys. Rev. Lett. **47**, 1665 (1981).

[6] S. R. Nagel, G. S. Grest, and A. Rahman, Phys. Today, **October**, 24 (1983).

[7] G. S. Grest, S. R. Nagel, A. Rahman, and T. W. Witten, Jr., J. Chem. Phys. **74**, 3532 (1981).

[8] J. Deisenhofer and W. Steigemann, Acta Crystallogr. B **31**, 238 (1975).

[9] H. J. C. Berendsen, J. P. M. Postma, W. F. van Gunsteren, A. DiNola, and J. R. Hank, J. Chem. Phys. **81**, 3684 (1984).

[10] J. A. Board, Jr., J. W. Causey, J. F. Leathrum, Jr., A. Windemuth, and K. Schulten, Chem. Phys. Lett. **198**, 89 (1992).

[11] A. Windemuth and K. Schulten, Mol. Simul. **5**, 353 (1991).

[12] B. R. Brooks, R. E. Bruccoleri, B. D. Olafson, D. J. States, S. Swaminathan, and M. Karplus, J. Comput. Chem. **4**, 187 (1983).

[13] A. MacKerell *et al.* (to be published).

[14] T. Noguti and N. Gō, Nature **296**, 776 (1982).

[15] B. R. Brooks and M. Karplus, Proc. Natl. Acad. Sci. U.S.A. **80**, 6571 (1983).

[16] M. Levitt, C. Sander, and P. S. Stern, J. Mol. Biol. **181**, 423 (1985).

[17] R. M. Levy, D. Perahia, and M. Karplus, Proc. Natl. Acad. Sci. U.S.A. **79**, 1346 (1982).

[18] D. Xu and K. Schulten (in preparation).

[19] E. B. Wilson, J. C. Decius, and P. C. Cross, *Molecular Vibrations* (Dover, New York, 1980).

[20] L. Rayleigh, *Scientific Papers* (Cambridge University Press, Cambridge, England, 1899–1920), Vol. I, p. 491 and Vol. IV, p. 370.

[21] L. Rayleigh, *The Theory of Sound*, 2nd ed. (MacMillan, London, 1894), Vol. I.

[22] A. Windemuth and K. Schulten, Beckman Institute Technical Report No. TB-91-19, University of Illinois, 1991.

[23] S. Cusack, J. Smith, J. Finney, B. Tider, and M. Karplus, J. Mol. Biol. **202**, 903 (1988).

[24] M. Abramowitz and I. A. Stegun, *Handbook of Mathematical Functions* (Dover, New York, 1965).

[25] W. Nadler, Proc. Natl. Acad. Sci. U.S.A. **84**, 7933 (1987).

[26] S. R. Nagel, A. Brunger, K. Schulten, M. Karplus, G. S. Grest, and A. Rahman, Phys. Rev. Lett. **53**, 368 (1984).

[27] C. Kittel, *Elementary Statistical Physics* (Wiley, Berlin, 1985).

[28] O. M. Becker and M. Karplus (to be published).

[29] J. Smith, K. Kuczera, and M. Karplus, Proc. Natl. Acad. Sci. U.S.A. **87**, 1601 (1990).

[30] D. Xu and K. Schulten, J. Chem. Phys. **103**, 3124 (1995).

[31] N. G. van Kampen, *Stochastic Processes in Physics and Chemistry* (North-Holland, Amsterdam, 1992).